



**HAL**  
open science

## High-resolution infrared spectroscopy of diacetylene below 1000 cm<sup>-1</sup>

Luca Bizzocchi, Filippo Tamassia, Claudio Degli Esposti, Luciano Fusina,  
Elisabetta Canè, Luca Dore

► **To cite this version:**

Luca Bizzocchi, Filippo Tamassia, Claudio Degli Esposti, Luciano Fusina, Elisabetta Canè, et al..  
High-resolution infrared spectroscopy of diacetylene below 1000 cm<sup>-1</sup>. *Molecular Physics*, 2011, pp.1.  
10.1080/00268976.2011.604646 . hal-00723631

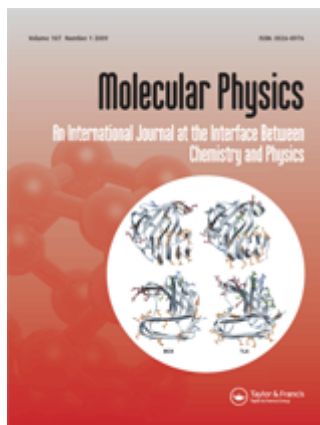
**HAL Id: hal-00723631**

**<https://hal.science/hal-00723631>**

Submitted on 12 Aug 2012

**HAL** is a multi-disciplinary open access archive for the deposit and dissemination of scientific research documents, whether they are published or not. The documents may come from teaching and research institutions in France or abroad, or from public or private research centers.

L'archive ouverte pluridisciplinaire **HAL**, est destinée au dépôt et à la diffusion de documents scientifiques de niveau recherche, publiés ou non, émanant des établissements d'enseignement et de recherche français ou étrangers, des laboratoires publics ou privés.



## High-resolution infrared spectroscopy of diacetylene below 1000 $\text{cm}^{-1}$

Journal:	<i>Molecular Physics</i>
Manuscript ID:	TMPH-2011-0139.R1
Manuscript Type:	Special Issue Paper - Dijon HRMS
Date Submitted by the Author:	25-Jun-2011
Complete List of Authors:	Bizzocchi, Luca; CAAUL, Observatório Astronómico de Lisboa Tamassia, Filippo; Università di Bologna, Dipartimento di Chimica Fisica e Inorganica Degli Esposti, Claudio; University of Bologna, Dipartimento di Chimica "G. Ciamician" fusina, luciano; Università di Bologna, Dipartimento di Chimica Fisica e Inorganica Canè, Elisabetta; Facoltà di Chimica Industriale, Università di Bologna, Dipartimento di Chimica Fisica e Inorganica Dore, Luca; University of Bologna, Dipartimento di Chimica "G. Ciamician"
Keywords:	Vibration-rotation bands, Diacetylene, Hot bands, Anharmonicity constants, Resonances
Note: The following files were submitted by the author for peer review, but cannot be converted to PDF. You must view these files (e.g. movies) online.	
source files.zip	

1  
2  
3  
4  
5  
6  
7  
8  
9  
10  
11  
12  
13  
14  
15  
16  
17  
18  
19  
20  
21  
22  
23  
24  
25  
26  
27  
28  
29  
30  
31  
32  
33  
34  
35  
36  
37  
38  
39  
40  
41  
42  
43  
44  
45  
46  
47  
48  
49  
50  
51  
52  
53  
54  
55  
56  
57  
58  
59  
60

SCHOLARONE™  
Manuscripts

For Peer Review Only

## RESEARCH ARTICLE

High-resolution infrared spectroscopy of diacetylene below  
1000 cm<sup>-1</sup>,†Luca Bizzocchi<sup>a,\*</sup>, Filippo Tamassia<sup>b</sup>, Claudio Degli Esposti<sup>c</sup>, Luciano Fusina<sup>b</sup>,  
Elisabetta Canè<sup>b</sup>, and Luca Dore<sup>c</sup><sup>a</sup>CAAUL, Observatório Astronómico de Lisboa, Tapada da Ajuda, 1349-018, Lisboa  
(Portugal); <sup>b</sup>Dipartimento di Chimica-Fisica ed Inorganica, Università di Bologna,  
Viale del Risorgimento 4, 40136 Bologna (Italy); <sup>c</sup>Dipartimento di Chimica “G.  
Ciamician”, Università di Bologna, via F. Selmi 2, 40126 Bologna (Italy)

(15 May 2011)

The infrared spectrum of diacetylene has been recorded at high resolution between 500 and 1000 cm<sup>-1</sup> by Fourier transform spectroscopy. More than 1200 transitions were assigned to 5 bands: the  $\nu_8$  fundamental, the  $\nu_7 + \nu_9$  combination, and the  $\nu_3 - \nu_9$  difference bands as well as the most intense  $\nu_8 + \nu_9 - \nu_9$  and  $\nu_7 + 2\nu_9 - \nu_9$  hot bands. The data were analysed together with the previously recorded millimetre-wave lines for the  $\nu_8 - \nu_6$  and  $\nu_8 + \nu_9 - (\nu_6 + \nu_9)$  difference bands. Rotational and vibrational *l*-type resonances, together with the cubic anharmonic interactions which couple the  $v_3 = 1$  stretching state with the  $v_8 = v_9 = 1$  combination and  $v_7 = 2$  overtone states have been considered in the least-squares fits to the observed wavenumbers in order to derive reliable spectroscopic parameters. The spectral analyses deliver very precise  $B_0$  and  $D_0$  parameters and experimental values of the anharmonicity constants for the bending–bending combination states of diacetylene below 1000 cm<sup>-1</sup>.

**Keywords:** Vibration-rotation bands; Diacetylene; Hot bands; Anharmonicity constants; Resonances

## 1. Introduction

Diacetylene (C<sub>4</sub>H<sub>2</sub>) is the simplest member of the family of poly-acetylene compounds and is a molecule of relevant astrophysical interest. It plays an important role in the stratospheres of the giant planets and their moons (see e.g., Ref. [1, 2]) acting as a UV shield analogously to O<sub>3</sub> in the Earth's atmosphere [3]. Like ozone, C<sub>4</sub>H<sub>2</sub> is photochemically reactive and it is thought to be a major source of the larger hydrocarbons, which then form the organic aerosols (tholines) characteristic of the reducing atmospheres of these solar system bodies [4]. Diacetylene has also been detected in the dusty envelopes of the C-rich proto-planetary nebula CRL 618 [5], and even outside the galaxy in a similar object embedded in the Large Magellanic Cloud [6]. Being centrosymmetric, C<sub>4</sub>H<sub>2</sub> has no permanent dipole moment, thus searches for this species in astrophysical environments rely on its mid infrared spectrum, in particular the strong  $\nu_8$  perpendicular band at 16  $\mu$ m, even if detection of the weaker bending fundamental  $\nu_9$  [1] and of the combination  $\nu_6 + \nu_8$  [5] was also reported.

†Dedicated to Prof. Gianfranco Di Lonardo.

\*Corresponding author. Email: bizzocchi@oal.ul.pt

1 The vibrational spectrum of diacetylene was the subject of extensive infrared and  
2 Raman investigations (see Ref. [7] and references therein). Several high-resolution  
3 studies of the infrared active bands have been performed. The  $\nu_4$  and  $\nu_5$  band  
4 systems were investigated by Guelachvili et al. [8], whereas the unusually strong  
5  $\nu_6 + \nu_8$  combination band at ca.  $1250\text{ cm}^{-1}$  has been investigated by Matsumura  
6 et al. [9] by Stark modulation infrared diode laser spectroscopy and, later, by  
7 McNaughton et al. [10] with a Fourier transform infrared (FTIR) spectrometer.  
8 Below  $1000\text{ cm}^{-1}$  the infrared spectrum of diacetylene is characterised by the strong  
9  $\nu_9$  and  $\nu_8$  bands, which were the subject of the high resolution study by Arié  
10 and Johns [11]. They reported band constants for the  $\nu_9$  and  $\nu_8$  fundamentals,  
11 and for several hot bands originating from the low lying  $\nu_9$  bending mode and  
12 its overtones. However, they were unable to obtain a satisfactory analysis for the  
13  $\nu_8 + \nu_9 - \nu_9$  hot band due to an anharmonic interaction coupling the  $v_8 = v_9 = 1$   
14 bending combination state and the  $v_3 = 1$  stretching state.  
15

16 In diacetylene, the dipole moment second derivatives with respect to the  $\text{C}\equiv\text{C}-\text{H}$   
17 bending curvilinear coordinates are large, and this produces enhanced transition  
18 moments for the overtone, combination, and difference bands involving the  $v_6$  and  
19  $v_8$  quanta [12, 13]. For instance, the intensity of the  $\nu_8 - \nu_6$  band is substantially  
20 enhanced and, since its origin is located below 100 GHz, it provides a mean of  
21 detecting diacetylene through millimetre-wave (mm-wave) spectroscopy [14, 15].  
22 Very recently, we have extended to the submillimetre-wave (submm-wave) region  
23 the study of this band and of its  $\nu_8 + \nu_9 - (\nu_6 + \nu_9)$  hot band, performing a complete  
24 analysis of the  $l$ -type resonance effects and of the above mentioned anharmonic  
25 interaction affecting the  $v_8 = v_9 = 1$  state [16]. However, no direct information on  
26 the  $v_3 = 1$  state could be obtained from mm-wave spectra, thus the spectroscopic  
27 constants of this level had to be estimated from recent theoretical calculations [17,  
28 18].  
29

30 In this paper we present the results obtained from the analysis of the infrared  
31 spectrum of diacetylene in the  $500\text{--}1000\text{ cm}^{-1}$  range, recorded using an FTIR spec-  
32 trometer. Besides the reinvestigation of the  $\nu_8$  band system, we could identify the  
33 previously unreported  $\nu_7 + \nu_9$  combination band at ca.  $700\text{ cm}^{-1}$ , together with the  
34 strong  $\nu_9$ -associated hot bands  $\nu_8 + \nu_9 - \nu_9$  and  $\nu_7 + 2\nu_9 - \nu_9$ . In addition, the very  
35 weak and previously unreported  $\nu_3 - \nu_9$  difference band — which provides direct  
36 information on the  $v_3 = 1$  state — was also identified and analysed, leading to a  
37 comprehensive analysis of the lowest diacetylene resonance system.  
38

39 The model adopted for the analysis includes the rotational and vibrational  $l$ -type  
40 resonances active between the various  $l$ -sublevels of the multiple bending excited  
41 states, and also considers the two anharmonic interactions which couple  $v_3 = 1$  with  
42 the  $v_8 = v_9 = 1$  combination and the  $v_7 = 2$  overtone states through the normal  
43 coordinates cubic potential constants  $\phi_{389}$  and  $\phi_{377}$ . The previously recorded mm-  
44 wave transition frequencies [16] were also taken into account in order to obtain the  
45 best set of spectroscopic parameters for the ground state and for the  $v_6 = 1$  and  
46  $v_8 = 1$  bending states.  
47

48 The results of the spectral analyses also provide a comprehensive set of anhar-  
49 monicity constants for the three bending–bending combination states of diacetylene  
50 located below  $1000\text{ cm}^{-1}$ , namely  $v_8 = v_9 = 1$ ,  $v_6 = v_9 = 1$ , and  $v_7 = v_9 = 1$ . The  
51 accurate treatment of the anharmonic resonances has enabled the determination of  
52 de-perturbed molecular parameters, whose values can be compared with the results  
53 of the recent high-level *ab initio* calculations [17, 18].  
54  
55  
56  
57  
58  
59  
60

## 2. Experimental details

Diacetylene was prepared by reacting commercially available 1,4-dichloro-2-butynes with aqueous NaOH using the procedure described by Armitage et al. [19]. High resolution IR spectra were recorded in the 500–1000 cm<sup>-1</sup> range using a BOMEM DA3.002 Fourier transform spectrometer at the University of Bologna. The interferometer was equipped with a KBr beam splitter, a Globar source, and a HgCdTe detector. An optical path length of 0.18 m was adopted with sample pressures of 270 Pa and 27 Pa. The attained unapodised resolution was 0.004 cm<sup>-1</sup>. A large number of scans were co-added in order to improve the signal-to-noise ratio: in total, 780 scans were recorded for the low pressure spectrum whereas 880 scans were co-added for the high pressure spectrum. An overview of the recorded IR spectrum of diacetylene between 590 and 730 cm<sup>-1</sup> is shown in Figure 1 together with the assignments of the most prominent spectral features. Ro-vibrational transitions of H<sub>2</sub>O [20] and CO<sub>2</sub> were used for calibration. The most accurate determination of the CO<sub>2</sub> transitions used as reference ( $\nu_2$  fundamental band) was performed by J.W.C. Johns, M. Noël and T.L. Tan. The line list was received as a private communication but, to our knowledge, the paper has not been published yet. The average precision of our measurements was estimated to be around 0.004 cm<sup>-1</sup>.

## 3. Observed spectra and analysis

In the present work, we have investigated the ro-vibrational bands  $\nu_8$ ,  $\nu_7 + \nu_9$ ,  $\nu_8 + \nu_9 - \nu_9$ ,  $\nu_7 + 2\nu_9 - \nu_9$ , and  $\nu_3 - \nu_9$ . The IR data have been analysed together with the previous mm-wave measurements of the  $\nu_8 - \nu_6$  and  $\nu_8 + \nu_9 - (\nu_6 + \nu_9)$  bands [16], so that our analyses deal with a manifold of states involving excitation of the  $\nu_3$  stretch ( $\Sigma_g^+$ ) and all the four bending quanta ( $\nu_6, \nu_7, \nu_8, \nu_9$ ). **A list of the normal mode fundamentals is reported in Ref. [8]. The reader is also referred to Ref. [18] for a comprehensive description of the internal symmetry coordinates of diacetylene.**

Diacetylene has two equivalent hydrogen nuclei and two pairs of equivalent carbon nuclei which are interchanged by the  $C_2$  symmetry operation. As a result, the ro-vibrational lines show a 3:1 intensity alternation due to the spin statistical weights. Table 1 summarises the spin multiplicity rules which apply for the vibrational states involved in the investigated bands.

The spectra were analysed by expressing each ro-vibrational energy term using the formalism originally developed by Yamada and co-workers [21, 22], and employed previously to fit the excited state rotational spectra of several carbon chains (see for example Ref. [23]). Briefly, the ro-vibrational Hamiltonian is first represented using the symmetric top basis functions  $|v_3, v_6^{l_6}, v_7^{l_7}, v_8^{l_8}, v_9^{l_9}; J, k\rangle$ , with  $k = l_6 + l_7 + l_8 + l_9$ . Employing the simplified notation  $|l_6, l_7, l_8, l_9; k\rangle$  the elements of the Hamiltonian matrix which are diagonal in the quantum numbers  $v_t$  and  $l_t$  are:

$$\begin{aligned} \langle l_6, l_7, l_8, l_9; k | \hat{H} | l_6, l_7, l_8, l_9; k \rangle = & G_v + \sum_{t=6,9} x_{L(tt)} l_t^2 + \sum_{t'>t=6,9} x_{L(tt')} l_t l_{t'} \\ & + \left\{ B_v + \sum_{t=6,9} d_{JL(tt)} l_t^2 + \sum_{t'>t=6,9} d_{JL(tt')} l_t l_{t'} \right\} \{ J(J+1) - k^2 \} \\ & - D_v \{ J(J+1) - k^2 \}^2 + H_v \{ J(J+1) - k^2 \}^3, \end{aligned} \quad (1)$$

where  $G_v$  is the “pure” vibrational energy of the  $|v_6, v_7, v_8, v_9\rangle$  state and includes the appropriate anharmonic corrections. The origin of a ro-vibrational band,  $\nu_0$ , is then given as  $G'_v - G''_v$ . The off-diagonal rotational  $l$ -type doubling terms ( $\Delta l_t \pm 2$ ,  $|\Delta k| = 2$ ) have the general form:

$$\begin{aligned} \langle l_t \pm 2, l_{t'}; k \pm 2 | \hat{H} | l_t, l_{t'}; k \rangle &= \frac{1}{4} \{ q_t + q_{tJ} J(J+1) \} \\ &\times \sqrt{(v_t \mp l_t)(v_t \pm l_t + 2)} \\ &\times \sqrt{[J(J+1) - k(k \pm 1)][J(J+1) - (k \pm 1)(k \pm 2)]}; \end{aligned} \quad (2)$$

whereas the off-diagonal vibrational  $l$ -type doubling terms ( $\Delta l_t \pm 2$ ,  $\Delta l_{t'} \mp 2$ ,  $\Delta k = 0$ ) are given by the expression:

$$\begin{aligned} \langle l_t \pm 2, l_{t'} \mp 2; k | \hat{H} | l_t, l_{t'}; k \rangle &= \frac{1}{4} \{ r_{tt'} + r_{tt'J} J(J+1) \} \\ &\times \sqrt{(v_t \mp l_t)(v_t \pm l_t + 2)(v_{t'} \mp l_{t'} + 2)(v_{t'} \pm l_{t'})}. \end{aligned} \quad (3)$$

The resulting energy matrix is factorised into symmetric and antisymmetric blocks adopting the following Wang-type linear combinations of wavefunctions [21].

$$\begin{aligned} |v_3, v_6^{l_6}, v_7^{l_7}, v_8^{l_8}, v_9^{l_9}; k\rangle_{\pm} \\ = \frac{1}{\sqrt{2}} \{ |v_3, v_6^{l_6}, v_7^{l_7}, v_8^{l_8}, v_9^{l_9}; k\rangle \pm |v_3, v_6^{-l_6}, v_7^{-l_7}, v_8^{-l_8}, v_9^{-l_9}; -k\rangle \} \end{aligned} \quad (4a)$$

$$|v_3, v_6^0, v_7^0, v_8^0, v_9^0; 0\rangle_{+} = |v_3, v_6^0, v_7^0, v_8^0, v_9^0; 0\rangle \quad (4b)$$

Any sublevel belonging to a given vibrational state can thus be labelled through its  $k$  value and by the ‘+’ or ‘-’ subscripts which designate the sign of the symmetrised linear combination or, alternatively, with the  $e$ ,  $f$  parity labels [24] using the correspondence  $+ \leftrightarrow e$ ,  $- \leftrightarrow f$  for even  $k$  and vice versa for odd  $k$ .

As mentioned in the Introduction, the three-state resonance system  $v_3 = 1 \sim v_8 = v_9 = 1 \sim v_7 = 2$  has been considered in the present work, and thus two Fermi-type ( $\Delta k = 0$ ) anharmonic interaction terms were included in the Hamiltonian. The corresponding off-diagonal matrix elements in the symmetrised basis are expressed by [25]:

$$\begin{aligned} {}_e \langle 1, 0^0, 0^0, 0^0, 0^0; J, 0 | \hat{H}_{30} | 0, 0^0, 0^0, 1^1, 1^{-1}; J, 0 \rangle_e \\ = W_{389} + W_{389J} J(J+1) = \frac{1}{2} \phi_{389} + W_{389J} J(J+1). \end{aligned} \quad (5)$$

$$\begin{aligned} {}_e \langle 1, 0^0, 0^0, 0^0, 0^0; J, 0 | \hat{H}_{30} | 0, 0^0, 2^0, 0^0, 0^0; J, 0 \rangle_e \\ = W_{377} + W_{377J} J(J+1) = \frac{\sqrt{2}}{4} \phi_{377} + W_{377J} J(J+1). \end{aligned} \quad (6)$$

Over 1200 ro-vibrational transitions have been measured, and the complete list of analysed data is available as electronic supplementary material. Some details dealing with the analyses performed for the various bands are given in the following subsections.

### 3.1. The $\nu_8$ fundamental band

The  $\nu_8 = 1$  ( $\Pi_u$ ) state has two  $|k| = 1$  ro-vibrational sublevels, thus  $\nu_8$  is a perpendicular band whose transitions connect  $\Pi_u^e \leftarrow \Sigma_g^{+,e}$  levels in the  $P, R$  branches and  $\Pi_u^f \leftarrow \Sigma_g^{+,e}$  levels in the  $Q$  branch. Making use of the spectroscopic constants of Ref. [11], the assignment of the IR lines was straightforward: we measured a total of 261 transitions, up to  $P(105)$ ,  $R(109)$ , and  $Q(81)$ . These data were analysed together with our previous mm-wave ro-vibrational frequencies of the  $\nu_8 - \nu_6$  difference band, allowing to simultaneously determine of the spectroscopic parameters of the ground and of the  $\nu_6 = 1$  and  $\nu_8 = 1$  states.

The analysis was performed by expressing the ro-vibrational energy levels through Eqs. (1) and (2). A proper weighting factor ( $w = 1/\sigma^2$ ) was assigned to each datum, in order to take into account the different measurement precisions. The mm-wave lines were included in the data sets retaining the same weighting scheme already used in the previous work [16], whereas  $\sigma = 5 \times 10^{-4} \text{ cm}^{-1}$  was adopted for the present IR wavenumbers. The results of the least-squares fit are reported in Table 2

The inclusion in the data set of the very precise mm-wave data was beneficial to reduce significantly the correlations between the lower and upper state parameters of the  $\nu_8$  band. Improved values of the ground state rotational and quartic centrifugal distortion constants of diacetylene were obtained. Compared with the previous best literature values of Ref. [11], i.e.  $B_0 = 4389.3019(38)$  MHz and  $D_0 = 0.47004(54)$  kHz, our precision is five and ten times better, respectively.

### 3.2. The $\nu_8 + \nu_9 - \nu_9$ hot band and $\nu_3 - \nu_9$ difference band

The  $\nu_8 = \nu_9 = 1$  state consists of three sub-states:  $\Sigma_g^+$  and  $\Sigma_g^-$  having  $k = 0$  (species  $e$  and  $f$ , respectively) and the doubly degenerate  $\Pi_g$  with  $|k| = 2$ , split by ro-vibrational  $l$ -type resonances into  $e, f$  doublets. The  $\nu_8 + \nu_9 - \nu_9$  hot band has a perpendicular structure with  $\Delta k = \pm 1$ , and selection rules  $e \leftarrow e, f \leftarrow f$  for  $P$ - and  $R$ -type transitions, and  $e \leftrightarrow f$  for  $Q$  branch lines.

This band was first studied by Arié and Johns [11]. However, they could not attain a satisfactory fit of the experimental wavenumbers and, even using a limited data set ( $J \leq 50$ ), the root mean square of the residuals remained substantially larger than the experimental precision ( $rms_{\text{IR}} \sim 0.007 \text{ cm}^{-1}$ ). According to Matsumura and Tanaka [15] the anomaly was attributed to an anharmonic resonance between the  $0^e$  ( $\Sigma_g^+$ ) sublevel of the  $\nu_8 = \nu_9 = 1$  state and the nearby  $\nu_3 = 1$  ( $\Sigma_g^+$ ) C-C stretching state. This interaction was actually considered in our recent mm-wave investigation [16] where, with the help of the recent theoretical results [17, 18], we achieved a satisfactory analysis of the  $\nu_8 + \nu_9 - (\nu_6 + \nu_9)$  band.

In the present work we have also identified the weak spectrum of the  $\nu_3 - \nu_9$  difference band thus gaining direct information on the  $\nu_3 = 1$  state. Using the values of the  $\nu_3$  and  $\nu_9$  fundamentals reported in Ref. [8],  $\nu_3 - \nu_9$  is calculated at ca.  $652 \text{ cm}^{-1}$ . Fortunately, in that region the intensity of the  $\nu_8$  band system is rapidly decreasing. Its transitions vanish almost completely at wavenumbers higher than  $660 \text{ cm}^{-1}$ , where the  $\nu_3 - \nu_9$   $R$ -branch lines should have their maximum intensity. A regular sequence of lines showing the characteristic intensity alternation was readily found. The assignment of the  $R$ -branch allowed to locate the  $Q$  branch, whose lines are widely spaced toward lower wavenumbers, due to the large negative value of the  $B_v(\nu_3 = 1) - B_v(\nu_9 = 1)$  difference. A portion of the  $Q$  branch of the  $\nu_3 - \nu_9$  band spectrum is shown in Figure 2. Despite the spectral congestion we could assign 60 transitions up to  $R(60)$ ,  $Q(57)$ , and  $P(32)$ . They were analysed simultaneously

with 567 lines assigned to the  $\nu_8 + \nu_9 - \nu_9$  hot band (spanning  $J$  interval 5–80) and with 158 mm-wave transitions of the  $\nu_8 + \nu_9 - (\nu_6 + \nu_9)$  difference band [16]. The weighting scheme was similar to that adopted for the simultaneous fit of  $\nu_8$  and  $\nu_8 - \nu_6$  described in the previous subsection: experimental uncertainties ( $\sigma$ ) for mm-wave lines were as in the original paper [16], while  $\sigma = 1 \times 10^{-3} \text{ cm}^{-1}$  was assigned to each infrared line belonging to the  $\nu_8 + \nu_9 - \nu_9$  and  $\nu_3 - \nu_9$  bands.

The ro-vibrational level energies were expressed using Eqs. (1)–(3), where the  $l$ -type resonance term of Eq. (3) applies for the  $v_8 = v_9 = 1$  and  $v_6 = v_9 = 1$  combination states only. Initially, the analysis of the resonance followed the same scheme adopted for the  $\nu_8 + \nu_9 - (\nu_6 + \nu_9)$  band [16], i.e. we included in the calculations the matrix elements of Eq. (5) coupling the  $v_3 = 1$  state and the  $(v_8 = v_9 = 1)^{0e}$  sublevel. The interaction constant of  $W_{389}$  was fixed at the value derived from the *ab initio*  $\phi_{389}$  normal coordinate cubic force constant ( $13.49 \text{ cm}^{-1}$ , Ref. [26]), while the  $G_v(v_3 = 1)$  vibrational energy was adjusted in the least-squares fit in order to reproduce the observed  $\nu_3 - \nu_9$  line positions.

The fit was very satisfactory, but the value of the  $B_v$  rotational constant of the  $v_3 = 1$  state was anomalously large. The corresponding  $\alpha_3$  was ca. 3.1 MHz, much smaller than the *ab initio* computed value of 9.4 MHz [18]. This suggested that the de-perturbation of the  $v_3 = 1$  state energy was incomplete and that it was still affected by a mixing with a vibrational state characterised by a larger rotational constant. The only state which can be coupled to  $v_3 = 1$  through a first-order (cubic) anharmonic resonance is  $v_7 = 2$ ,  $k = 0^e$  ( $\Sigma_g^+$ ), which is at ca.  $75 \text{ cm}^{-1}$  higher energy and interacts through the normal coordinate force constant  $\phi_{377}$ , whose theoretical value is  $113.87 \text{ cm}^{-1}$  [26]. The same scheme of interactions has previously been found for other similar carbon chains, such as HCCCN [27], HCCNC [28] and HCCCP [29], where the lowest-energy stretching state is coupled, through cubic interactions, with nearby bending overtone and combination states.

The analysis was thus performed considering the  $v_3 = 1$ ,  $v_8 = v_9 = 1$ , and  $v_7 = 2$  states simultaneously in order to take into account the resonance effects as completely as possible. The energy level diagram for the three interacting states is illustrated in Figure 3. We adjusted the upper state parameters, keeping the constants of the lower  $v_9 = 1$  state fixed at the values derived from the analysis of the  $\nu_9$  band [11]. The rotational parameters  $B_v$ ,  $D_v$ , and  $q_7$  of the unobserved  $v_7 = 2$  state were evaluated from the experimental results for the  $\nu_7$  fundamental [8]; whereas a suitable assumption for the anharmonicity constant  $x_{L(77)}$  was obtained by removing from the theoretical value [18] the relevant near-singular term (see Discussion).

The main off-diagonal resonance parameters  $W_{389}$  and  $W_{377}$  were constrained to the values derived from the corresponding cubic force constants [17, 26], whereas the unperturbed energy difference between the  $v_3 = 1$  and the  $v_7 = 2$  states was assumed equal to the quantity  $2\omega_7 - \omega_3$  [18]. Both the centrifugal corrections  $W_{389J}$  and  $W_{377J}$  (see Eqs. (5) and (6)) were found to be important in reproducing the rotational mixing caused by the  $v_3 \sim v_8 + v_9$  and  $v_3 \sim 2v_7$  resonances. While  $W_{389J}$  could be determined,  $W_{377J}$  had to be constrained to a suitable value. As already pointed out, the energy level structure of the lowest resonance system of diacetylene is analogue to that of the isoelectronic molecule HCCCN, so it is likely that their molecular parameters show some similarities. From Ref. [30] we derived a scaled  $W_{377J}$  value of -1.41 MHz (see Discussion for the details), which was constrained in the final analysis. The spectroscopic constants determined by the least-squares fit are collected in Table 3. **The overall fit quality ( $rms_{\text{IR}} = 1.4 \times 10^{-3} \text{ cm}^{-1}$ ) is satisfactory considering that the data set includes the very weak  $\nu_3 - \nu_9$  band transitions, whose positions are clearly affected by**

1 **larger measurements errors.** The derived unperturbed value of the  $B_v(v_3 = 1)$   
 2 rotational constant yields  $\alpha_3 = 9.325$  MHz which compares very well with the *ab*  
 3 *initio* computed value of 9.395 MHz [18]. **A similar agreement (within 1%)**  
 4 **is observed for the  $\alpha_9$  vibration-rotation interaction constants, which in**  
 5 **turn derives from the analysis of unperturbed vibrational levels [11].**  
 6  
 7  
 8

### 9 3.3. The $\nu_7 + \nu_9$ combination band

10 The spectral survey carried out in the present investigation allowed us to identify  
 11 the  $\nu_7 + \nu_9$ ,  $\Sigma_u^+ \leftarrow \Sigma_g^+$  parallel band, which appears as a weak but nevertheless clear  
 12 feature in the high pressure spectra (see Figure 1). Making use of the values of  $B_0$   
 13 and  $\Delta B = -(\alpha_7 + \alpha_9)$  (from this work and Refs. [8, 11]), we assigned 137 transitions  
 14 with  $J'$  up to 75 for both *P*- and *R*-branches.  
 15

16 A rather high root mean square deviation,  $rms_{IR} \sim 0.008$  cm<sup>-1</sup>, and an anoma-  
 17 lously large value for the upper state  $D_v$  constant was obtained from the fit of  
 18 these data. This unsatisfactory result was due to the neglect of the *l*-type reso-  
 19 nance between the  $k = 0^e$  and  $k = 2^e$  sublevels of the  $v_7 = v_9 = 1$  state. A correct  
 20 treatment of this resonance requires the knowledge of the  $x_{L(79)}$  and  $r_{79}$  anhar-  
 21 monicity constants, as the observed  $\Delta k = 0$  transitions of the  $\nu_7 + \nu_9$  band cannot  
 22 provide information on the upper state manifold. These parameters were obtained  
 23 from the analysis of the associated  $\nu_7 + 2\nu_9 - \nu_9$  hot band (see next subsection),  
 24 thus allowing to characterise the ro-vibrational levels of the  $v_7 = v_9 = 1$  state as  
 25 described in the following.  
 26

27 The energy terms were expressed using Eqs. (1)–(3), and the fit was carried out  
 28 with the ground state constants fixed at the values derived in the present work (see  
 29 subsection 3.1). As for the *l*-type doubling constants  $q_7$ ,  $q_9$  and  $q_{9J}$  the literature  
 30 values of the  $v_7 = 1$  [8] and  $v_9 = 1$  [11] states were adopted. The  $x_{L(79)}$  and  $r_{79}$   
 31 parameters were from the fit of the  $\nu_7 + 2\nu_9 - \nu_9$  hot band. A new fit, carried out  
 32 adjusting the band origin,  $B_v$ , and  $D_v$  yielded a significantly smaller root mean  
 33 square deviation ( $rms_{IR} \sim 0.001$  cm<sup>-1</sup>). We then refined also  $x_{L(79)}$  in the final  
 34 analysis to reproduce accurately the magnitude of the *l*-type resonance effects.  
 35 The results of the final least-squares fit are gathered in Table 4. Besides the mere  
 36 improvement of the fit quality ( $rms_{IR} = 4 \times 10^{-4}$  cm<sup>-1</sup>), the effectiveness of the  
 37 treatment is supported by the value of  $D_v$  for the  $v_7 = v_9 = 1$  state, 0.5035 kHz,  
 38 in good agreement with that extrapolated from the singly excited bending states.  
 39  
 40  
 41

### 42 3.4. The $\nu_7 + 2\nu_9 - \nu_9$ hot band

43 The  $\nu_7 + 2\nu_9 - \nu_9$  hot band appears as a feature superimposed to the  $\nu_7 + \nu_9$   
 44 band. The intensity of its lines is ca. one third of that of the corresponding cold  
 45 band transitions, owing to the low energy of the  $v_9 = 1$  state ( $\sim 220$  cm<sup>-1</sup> [11]).  
 46 The  $(v_7 = 1, v_9 = 2)$  state is composed of three pairs of ro-vibrational sublevels,  
 47 which can be labelled as  $k = 3^{e,f}$  ( $\Phi_g$ ),  $k = 1^{e,f}$  ( $\Pi_g$ ), and  $k = -1^{e,f}$  ( $\Pi_g$ ). The  
 48  $k = 3^{e,f}$  and  $k = -1^{e,f}$  sublevels have  $|l_9| = 2$  and are separated from the  $k = 1^{e,f}$   
 49 sublevels by the anharmonic contribution  $x_{L(99)}l_9^2$ . On the other hand, the  $k = 3^{e,f}$   
 50 and  $k = -1^{e,f}$  sublevels are split symmetrically by the term  $x_{L(79)}l_7l_9$ , and finally  
 51 the degeneracy between each pair of *e, f* levels is lifted by vibrational and rotational  
 52 *l*-type resonance effects. Allowed  $\Delta k = 0$  transitions are observed between  $v_9 = 1$ ,  
 53  $k = 1^{e,f}$  and  $(v_7 = 1, v_9 = 2)$ ,  $k = 1^{e,f}$  sub-states. The spectrum consists of two  
 54 sequences of *e* and *f* lines rather than close doublets, owing to the large separation  
 55 of *e* and *f* components. We identified a total of 218 lines up to *P*(57) and *R*(67).  
 56  
 57  
 58

59 The analysis was carried out by expressing the energies of the ro-vibrational  
 60

1 levels through Eqs. (1)–(3), keeping the spectroscopic constants of the  $v_9 = 1$   
 2 state fixed at the literature values [11]. The excited-state constants  $q_7$  and  $x_{L(99)}$   
 3 were also assumed from the results of previous analyses [8, 11], whereas both the  
 4 anharmonicity constants  $x_{L(79)}$  and  $r_{79}$  were adjusted. In fact, our experimental  
 5 data are sensitive to both these parameters, since  $x_{L(79)}$  contributes to the energy  
 6 difference between the various  $k$  sub-states, and  $r_{79}$  is responsible for the vibrational  
 7  $l$ -type resonance between the  $k = 1$  and  $k = -1$  sub-states. The results of the least-  
 8 squares fit are reported in Table 5.  
 9

10  
 11  
 12 **4. Discussion**

13  
 14  
 15 In the present study we have determined several spectroscopic constants for a  
 16 number of states involved in vibrational and ro-vibrational resonances, due both  
 17 to the  $l$ -sublevel structure of the bending excited state and to accidental near-  
 18 degeneracies. In our spectral analyses, we succeeded in retrieving molecular pa-  
 19 rameters with unambiguous physical meaning. This is particularly relevant if one  
 20 aims at a meaningful comparison with the results of theoretical calculations. Due  
 21 to correlations between the model Hamiltonian parameters, not all the quantities  
 22 involved in the two anharmonic interactions analysed, i.e.  $v_3 \sim v_8 + v_9$  and  $v_3 \sim 2v_7$ ,  
 23 could be determined from the least-squares fits, so that a number of assumptions  
 24 had to be made. Whenever possible, the values of the parameters have been derived  
 25 from the experimental results for vibrational states at a lower level of excitation  
 26 (e.g.  $B_v$  and  $D_v$  for the unobserved  $v_7 = 2$  state) or from the most recent *ab initio*  
 27 anharmonic force field calculations [17, 18]. The only exception was the centrifugal  
 28 correction parameters  $W_{377J}$ , whose value was estimated empirically from the re-  
 29 sults of a global ro-vibrational analysis performed for the isoelectronic carbon chain  
 30 HCCC<sup>15</sup>N [30]. The resonance between  $v_4 = 1$  and  $v_6 = 2$ , present in HCCC<sup>15</sup>N,  
 31 is analogous to that between  $v_3 = 1$  and  $v_7 = 2$  which has been considered for di-  
 32 acetylene: Ref. [30] gives  $W_{466} = 43.03 \text{ cm}^{-1}$  and  $W_{466J} = -1.84 \text{ MHz}$ . According  
 33 to Aliev and Watson [31], it is possible to estimate the order of magnitude of an  
 34 Hamiltonian coefficient  $C_{mn}$  using  
 35

36  
 37  
 38 
$$C_{mn} \approx \kappa^{m+2n-2} \omega_{\text{vib}}, \quad (7)$$

39  
 40 where an approximate value of the Born–Oppenheimer expansion parameter  $\kappa \approx$   
 41 0.1 can be adopted for most vibrational problems. The ratio between  $W_{stt}$  and  $W_{sttJ}$   
 42 is of the order  $\kappa^{-4}$ , thus it is appropriate to derive an estimate for an unknown  
 43  $W_{377J}$  of diacetylene using the scaling equality:  
 44

45  
 46 
$$\left[ \frac{W_{377}(\text{HC}_4\text{H})}{W_{466}(\text{HC}_3\text{N})} \right]^4 = \frac{W_{377J}(\text{HC}_4\text{H})}{W_{466J}(\text{HC}_3\text{N})}. \quad (8)$$

47  
 48  
 49 Inserting in this relation the above mentioned HCCC<sup>15</sup>N values and  $W_{377} =$   
 50  $40.255 \text{ cm}^{-1}$  of diacetylene derived from the force field, one obtains  $W_{377J} =$   
 51  $-1.41 \text{ MHz}$  used in the present analysis. It is to be noted that we could have  
 52 omitted  $W_{377J}$  without degrading significantly the quality of the fit, but then we  
 53 would have been unable to model the correct rotational mixing produced by the  
 54 strongest anharmonic interaction  $v_3 = 1 \sim v_7 = 2$ , as already pointed out in a  
 55 number of previous studies (e.g. Ref. [32]). On the other hand, the effectiveness  
 56 of such a treatment can be assessed by the inspection of the converged values of  
 57 the rotational and quartic centrifugal distortion constants for the  $v_8 = v_9 = 1$  and  
 58  
 59  
 60

$v_6 = v_9 = 1$  states, which compare nicely with those obtained from the ground and singly excited state parameters. The derived  $\alpha_3$  exhibits a remarkable agreement with the *ab initio* value [18] (within 1%), and also  $D_v$  of the  $v_3 = 1$  state converges to a value slightly smaller than the ground state one, as expected for a stretching excited state of a well-behaved semi-rigid linear molecule.

We have also determined the  $x_{L(tt')}$  anharmonicity constants and the  $r_{tt'}$  vibrational  $l$ -type constants for the three bending–bending combination states of diacetylene below  $1000\text{ cm}^{-1}$ , i.e.  $v_8 = v_9 = 1$ ,  $v_6 = v_9 = 1$ , and  $v_7 = v_9 = 1$ . These parameters can be compared to the theoretically computed ones in Ref. [18] if one removes the near-singular terms entering in the second-order perturbation expressions in cases where  $2\omega_t \approx \omega_s$  or  $\omega_t + \omega_{t'} \approx \omega_s$  [33]. The relevant terms can be factored as follows:

$$x_{L(tt)} = x_{L(tt)}^* - \frac{1}{32}\phi_{stt}^2(2\omega_t - \omega_s)^{-1}, \quad (9)$$

$$x_{L(tt')} = x_{L(tt')}^* - \frac{1}{16}\phi_{stt'}^2(\omega_t + \omega_{t'} - \omega_s)^{-1}, \quad (10)$$

$$r_{tt'} = r_{tt'}^* + \frac{1}{8}\phi_{stt'}^2(\omega_t + \omega_{t'} - \omega_s)^{-1}, \quad (11)$$

where the asterisk at the superscript labels “de-perturbed” anharmonicity constants. Eq. (9) was used to compute the de-perturbed  $x_{L(77)}^*$  parameter from the theoretical  $x_{L(77)}$  prediction [18].  $x_{L(77)}^*$  was then fixed in the analysis of the polyad involving the  $v_7 = 2$  state (see subsection 3.2 and Table 3). The comparison between the experimentally derived and *ab initio* computed values of these constants is presented in Table 6. As can be seen, the agreement is satisfactory for  $x_{L(tt')}$ , but rather poor for the vibrational  $l$ -type parameters. This different behaviour was somewhat expected since the expression of  $r_{tt'}$  contains a semi-diagonal quartic potential constant of the type  $\phi_{tt't'}$ , whereas the  $x_{L(tt')}$  are defined in terms of the quadratic and cubic potential constants only. It is likely that high-order potential constants are affected by larger uncertainties, (usually not estimated in theoretical works), which then lead to less accurate predictions of the derived spectroscopic parameters.

This hypothesis seems to be supported by the energy difference between the  $k = 0^f$  and  $k = 2^f$  sublevels of the  $v_8 = v_9 = 1$  state, which are both unaffected by the anharmonic resonance. A spectral analysis limited to  $(v_8 = v_9 = 1)^{0f,2f}$  data gives  $E_{2^f} - E_{0^f} = 0.62\text{ cm}^{-1}$ . This difference equals, to a very good approximation, the sum  $2x_{L(89)} + r_{89} - 4B_v$ , in which the two near-singular terms included in  $x_{L(89)}$  and  $r_{89}$  cancel each other out. Using the *ab initio* calculated constants of [18] it results  $E_{2^f} - E_{0^f} = -0.09\text{ cm}^{-1}$ , which differs from the experimental value by  $0.71\text{ cm}^{-1}$  (i.e. 21.3 GHz), an amount close to the discrepancy between experimental and theoretical  $r_{89}$  values.

## 5. Conclusions

The present paper reports on the results of the accurate analysis of the ro-vibrational spectrum of diacetylene in the  $500\text{--}1000\text{ cm}^{-1}$  region. New infrared measurements allowed for the identification of the previously unreported  $\nu_7 + \nu_9$ ,  $\nu_7 + 2\nu_9 - \nu_9$ , and  $\nu_3 - \nu_9$  bands. Also, we reinvestigated the  $\nu_8$  fundamental and its associated  $\nu_8 + \nu_9 - \nu_9$  hot band, analysing these infrared data with the mm-wave transitions of the  $\nu_8 - \nu_6$  and  $\nu_8 + \nu_9 - (\nu_6 + \nu_9)$  difference bands [16].

The ro-vibrational treatment of this enlarged data set was performed using the linear molecule Hamiltonian developed by Yamada et al. [21], resulting in a single set of spectroscopic constants for each of the vibrational state involved in the investigated bands. The anharmonic resonances which couples the  $v_3 = 1$  (C–C stretch,  $\Sigma_g^+$ ) state with the  $\Sigma_g^+$  ( $k = 0^e$ ) sublevel of the  $v_8 = v_9 = 1$  and  $v_7 = 2$  states have been explicitly taken into account in the least-squares fit in order to obtain de-perturbed spectroscopic parameters having clear physical meaning.

This work also achieves the complete characterisation of the lowest bend–bend combination states  $v_8 = v_9 = 1$ ,  $v_6 = v_9 = 1$ , and  $v_7 = v_9 = 1$ , through the determination of their anharmonicity and vibrational  $l$ -type doubling constants  $x_{L(89)}^*$ ,  $x_{L(69)}$ ,  $x_{L(79)}$ ,  $r_{89}^*$ ,  $r_{79}$ , and  $r_{69}$ .

## Acknowledgements

The authors wish to thank M. Di Lauro for the preparation of the sample. Financial support from MIUR (PRIN 2007 funds, project “Trasferimenti di energia, carica e molecole in sistemi complessi”) and from the University of Bologna (RFO funds) is gratefully acknowledged. LB acknowledges support from the Science and Technology Foundation (FCT, Portugal) through the grant SFRH/BPD/62966/2009.

## References

- [1] V.G. Kunde, A.C. Aikin, R.A. Hanel, D.E. Jennings, W.C. Maguire and R.E. Samuelson, *Nature* **292**, 686 (1981).
- [2] Th. de Graauw, H. Feuchtgruber, B. Bézard, P. Drossart, Th. Encrenaz, D. A. Beintema, M. Griffin, A. Heras, M. Kessler, K. Leech, E. Lellouch, P. Morris, P. R. Roelfsema, M. Roos-Serote, A. Salama, B. Vandenbussche, E. A. Valentijn, G. R. Davis and D. A. Naylor, *Astron. Astrophys.* **321**, L13 (1997).
- [3] R.E. Bandy, C. Lakshminarayan, R.K. Frost and T.S. Zwier, *Science* **258**, 1630 (1992).
- [4] J.H. Waite Jr., D.T. Young, T.E. Cravens, A.J. Coates, F.J. Crary, B. Magee and J. Westlake, *Nature* **316**, 870 (2007).
- [5] J. Cernicharo, A.M. Heras, A.G.G.M. Tielens, J.R. Pardo, F. Herpin, M. Guélin and L.B.F.M. Waters, *Astrophys. J.* **546**, L123 (2001).
- [6] J. Bernard-Salas, E. Peeters, G.C. Sloan, J. Cami, S. Guiles and J.R. Houck, *Astrophys. J.* **652**, L29 (2006).
- [7] N.L. Owen, C.H. Smith and G.A. Williams, *J. Mol. Struct.* **161**, 33 (1987).
- [8] G. Guelachvili, A.M. Craig and D.A. Ramsay, *J. Mol. Spectrosc.* **105**, 156 (1984).
- [9] K. Matsumura, K. Kawaguchi, E. Hirota and T. Tanaka, *J. Mol. Spectrosc.* **118**, 530 (1986).
- [10] D. McNaughton and D.N. Bruget, *J. Mol. Struct.* **273**, 11 (1992).
- [11] E. Arié and J.W.C. Johns, *J. Mol. Spectrosc.* **155**, 195 (1992).
- [12] K. Matsumura and T. Tanaka, *J. Mol. Spectrosc.* **116**, 320 (1986).
- [13] K. Matsumura and T. Tanaka, *J. Mol. Spectrosc.* **116**, 334 (1986).
- [14] K. Matsumura, T. Etoh and T. Tanaka, *J. Mol. Spectrosc.* **90**, 106 (1981).
- [15] K. Matsumura and T. Tanaka, *J. Mol. Spectrosc.* **96**, 219 (1982).
- [16] L. Bizzocchi, C. Degli Esposti and L. Dore, *Mol. Phys.* **108**, 2315 (2010).
- [17] S. Thorwirth, M.E. Harding, D. Muders and J. Gauss, *J. Mol. Spectrosc.* **251**, 220 (2008).
- [18] A.C. Simmonett, H.F. Schaefer III and W.D. Allen, *J. Chem. Phys.* **130**, 044301 (2009).
- [19] J.B. Armitage, R.H. Jones and M.C. Whiting, *J. Chem. Soc.* p. 55 (1951).
- [20] R.A. Toth, *J. Opt. Soc. Am. B* **8**, 2236 (1991).
- [21] K.M.T. Yamada, F.W. Birss and M.R. Aliev, *J. Mol. Spectrosc.* **112**, 347 (1985).
- [22] M. Niederhoff and K.M.T. Yamada, *J. Mol. Spectrosc.* **157**, 182 (1993).
- [23] C. Degli Esposti, L. Bizzocchi, P. Botschwina, K.M.T. Yamada, G. Winnewisser, S. Thorwirth and P. Förster, *J. Mol. Spectrosc.* **230**, 185 (2005).
- [24] J.M. Brown, J.T. Hougen, K.P. Huber, J.W.C. Johns, I. Kopp, H. Lefebvre-Brion, A.J. Merer, D.A. Ramsay, J. Rostas and R.N. Zare, *J. Mol. Spectrosc.* **55**, 500 (1975).
- [25] T. Okabayashi, K. Tanaka and T. Tanaka, *J. Mol. Spectrosc.* **195**, 22 (1999).
- [26] S. Thorwirth, Private communication.
- [27] K.M.T. Yamada and R.A. Creswell, *J. Mol. Spectrosc.* **116**, 384 (1986).
- [28] C. Vigouroux, A. Fayt, A. Guarnieri, A. Huckauf, H. Bürger, D. Lentz and D. Preugschat, *J. Mol. Spectrosc.* **202**, 1 (2000).
- [29] L. Bizzocchi, C. Degli Esposti, L. Dore and G. Cazzoli, *J. Mol. Spectrosc.* **205**, 164 (2001).
- [30] A. Fayt, F. Willaert, J. Demaison, T. Starck, H. Mäder, G. Pawelke, E. B. Mkadmi and H. Bürger, *Chem. Phys.* **346**, 115 (2008).
- [31] M.R. Aliev and J.K.G. Watson, in *Molecular Spectroscopy: Modern Research*, edited by K. Narahari Rao, Vol. III (1985), pp. 1–67.

[32]L. Bizzocchi, C. Degli Esposti and C. Puzzarini, *Mol. Phys.* **104**, 2627 (2006).  
[33]D. Papoušek and M.R. Aliev, *Molecular vibrational-rotational spectra* (Elsevier, 1982).

For Peer Review Only

Table 1. Spin statistical weights of the ro-vibrational levels of diacetylene.

Inversion parity	parity label	even $J$	odd $J$
$g$	$\left\{ \begin{array}{l} e \\ f \end{array} \right.$	1	3
		3	1
$u$	$\left\{ \begin{array}{l} e \\ f \end{array} \right.$	3	1
		1	3

Table 2. Spectroscopic parameters determined by the analysis of the  $\nu_8$  fundamental and of the  $\nu_8 - \nu_6$  difference bands of diacetylene<sup>a</sup>.

Parameter	<i>ground state</i>	$\nu_8 = 1$	$\nu_6 = 1$
$G_v$ / $\text{cm}^{-1}$	0.0 <sup>b</sup>	628.040776(36)	625.643507(36)
$B_v$ / MHz	4389.29687(60)	4391.201952(52)	4391.327830(53)
$D_v$ / kHz	0.470150(61)	0.472111(19)	0.472085(20)
$H_v$ / mHz		0.0326(24) <sup>c</sup>	0.0326(24) <sup>c</sup>
$q_t$ / MHz		2.409552(64)	2.485126(64)
$q_{tJ}$ / Hz		-1.309(11)	-1.187(11)
$rms_{\text{IR}}$ / $\text{cm}^{-1}$		$2.5 \times 10^{-4}$	
$rms_{\text{mmw}}$ / kHz		22.5	

<sup>a</sup> The quantity in parentheses is one standard deviation in units of the last quoted digit.  
<sup>b</sup> Constrained.  
<sup>c</sup> Fitted as a mean value for both states.

Table 3. Spectroscopic parameters determined by the analysis of the  $\nu_8 + \nu_9 - \nu_9$  hot band and of the  $\nu_3 - \nu_9$ ,  $\nu_8 + \nu_9 - (\nu_6 + \nu_9)$  difference bands of diacetylene<sup>a</sup>.

Parameter	$\nu_9 = 1$	$\nu_8 = \nu_9 = 1$	$\nu_6 = \nu_9 = 1$	$\nu_3 = 1$	$\nu_7 = 2$	
$G_v$	/ $\text{cm}^{-1}$	219.974 <sup>b</sup>	848.365918(53)	845.655513(54)	888.36279(30)	962.96 <sup>d</sup>
$x_L^+(77)$	/GHz					-50.33 <sup>c,d</sup>
$x_{L(99)}$	/ GHz	17.702 <sup>b</sup>	17.702 <sup>b</sup>	17.702 <sup>b</sup>		
$x_{L(t9)}$	/ GHz		12.19037(72) <sup>c</sup>	15.87245(71)		
$B_v$	/ MHz	4401.8473 <sup>b</sup>	4403.70993(22)	4403.86433(20)	4379.9715(59)	4405.205 <sup>d</sup>
$d_{JL(99)}$	/ kHz	-17.1 <sup>b</sup>	-17.1 <sup>b</sup>	-17.1 <sup>b</sup>		
$d_{JL(t9)}$	/ kHz		0.0 <sup>d</sup>	-4.96(13)		
$D_v$	/ kHz	0.4883 <sup>b</sup>	0.490137(80)	0.490189(74)	0.46159(41)	0.47 <sup>d</sup>
$q_7$	/ MHz					3.131 <sup>d</sup>
$q_t$	/ MHz		2.50214(33)	2.50544(21)		
$q_{tJ}$	/ Hz		-1.309 <sup>d</sup>	-1.187 <sup>d</sup>		
$q_9$	/ MHz	6.155 <sup>b</sup>	6.21994(19)	6.155 <sup>b</sup>		
$q_{9J}$	/ Hz	-12.86 <sup>b</sup>	-12.86 <sup>b</sup>	-12.86 <sup>b</sup>		
$r_{t9}$	/ GHz		11.8226(16) <sup>c</sup>	0.2970(16)		
$r_{t9J}$	/ kHz		-27.98(27)	-5.61(11)		
$W_{389}$	/ $\text{cm}^{-1}$			6.746 <sup>d</sup>		
$W_{389J}$	/ MHz			-1.1569(11)		
$W_{377}$	/ $\text{cm}^{-1}$			40.255 <sup>d</sup>		
$W_{377J}$	/ MHz			-1.41 <sup>d</sup>		
$rms_{\text{IR}}$	/ $\text{cm}^{-1}$			$1.4 \times 10^{-3}$		
$rms_{\text{mmw}}$	/ kHz			33.4		

<sup>a</sup> The quantity in parentheses is one standard deviation in units of the last quoted digit.

<sup>b</sup> Fixed at the value of Ref. [11]

<sup>c</sup> Deperturbed constant, see text.

<sup>d</sup> Constrained, see text.

Table 4. Spectroscopic parameters determined by the analysis of the  $\nu_7 + \nu_9$  combination band of diacetylene<sup>a</sup>.

Parameter	ground state	$\nu_7 = \nu_9 = 1$	
$G_v$	/ $\text{cm}^{-1}$	$0.0^b$	701.8939(20)
$x_{L(77)}$	/ GHz		$0.0^b$
$x_{L(99)}$	/ GHz		17.702 <sup>c</sup>
$x_{L(79)}$	/ GHz		13.457(57)
$B_v$	/ MHz	4389.2969 <sup>b</sup>	4409.9697(85)
$d_{JL(99)}$	/ kHz		-17.1 <sup>c</sup>
$D_v$	/ kHz	0.4702 <sup>b</sup>	0.50351(49)
$q_7$	/ MHz		3.131 <sup>d</sup>
$q_9$	/ MHz		6.155 <sup>c</sup>
$q_{9J}$	/ Hz		-12.86 <sup>c</sup>
$r_{79}$	/ GHz		-13.193 <sup>b</sup>
$rms_{IR}$	/ $\text{cm}^{-1}$		$4.0 \times 10^{-4}$

<sup>a</sup> The quantity in parentheses is one standard deviation in units of the last quoted digit.

<sup>b</sup> Constrained, see text.

<sup>c</sup> Fixed at the value of Ref. [11].

<sup>d</sup> Fixed at the value of the  $\nu_7 = 1$  state, Ref. [8].

Table 5. Spectroscopic parameters determined by the analysis of the  $\nu_7 + 2\nu_9 - \nu_9$  hot band of diacetylene<sup>a</sup>.

Parameter	$\nu_9 = 1$	$\nu_7 = 1, \nu_9 = 2$
$G_v$ / $\text{cm}^{-1}$	219.974 <sup>b</sup>	920.9939(11)
$x_{L(77)}$ / GHz	0.0 <sup>c</sup>	0.0 <sup>c</sup>
$x_{L(99)}$ / GHz	17.702 <sup>b</sup>	17.702 <sup>b</sup>
$x_{L(79)}$ / GHz		15.71(11)
$B_v$ / MHz	4401.8473 <sup>b</sup>	4422.5999(34)
$d_{JL(99)}$ / kHz	-17.1 <sup>b</sup>	-17.1 <sup>b</sup>
$D_v$ / kHz	0.4883 <sup>b</sup>	0.54224(94)
$q_7$ / MHz		3.131 <sup>d</sup>
$q_9$ / MHz	6.155 <sup>b</sup>	6.155 <sup>b</sup>
$q_{9J}$ / Hz	-12.86 <sup>b</sup>	-12.86 <sup>b</sup>
$r_{79}$ / GHz		-13.193(63)
$rms_{\text{IR}}$ / $\text{cm}^{-1}$		$5.5 \times 10^{-4}$

<sup>a</sup> The quantity in parentheses is one standard deviation in units of the last quoted digit.

<sup>b</sup> Fixed at the value of Ref. [11].

<sup>c</sup> Constrained.

<sup>d</sup> Fixed at the value of the  $\nu_7 = 1$  state, Ref. [8].

Table 6. Comparison between experimental and computed anharmonicity constants for diacetylene<sup>a</sup>.

Parameter	experimental	<i>ab initio</i>
$x_{L(89)}^*$ / GHz	12.19	14.4
$x_{L(79)}$ / GHz	13.46	15.0
$x_{L(69)}$ / GHz	15.87	14.7
$r_{89}^*$ / GHz	11.82	-13.8
$r_{69}$ / GHz	0.297	3.9
$r_{79}$ / GHz	-13.19	-32.8

<sup>a</sup> Asterisks at the superscript label deperturbed constants (see text).

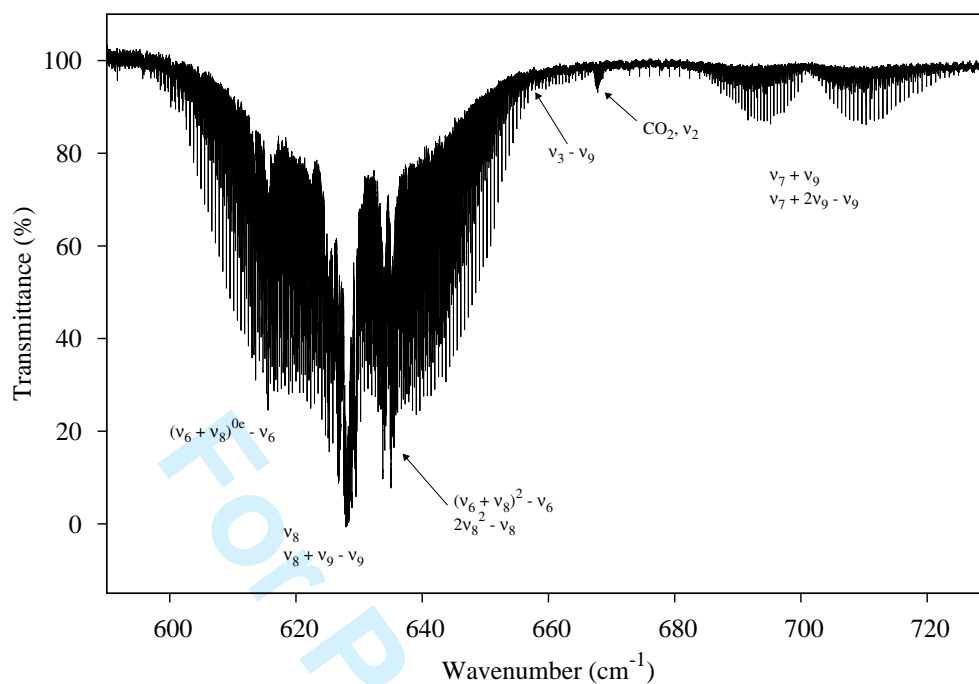


Figure 1. Overview of the infrared spectrum of diacetylene in the  $\nu_8$  band region. The assignment of some prominent features is indicated. Spectrum recorded at 270 Pa, 880 scans coadded for a final unapodised resolution of  $0.004 \text{ cm}^{-1}$ .

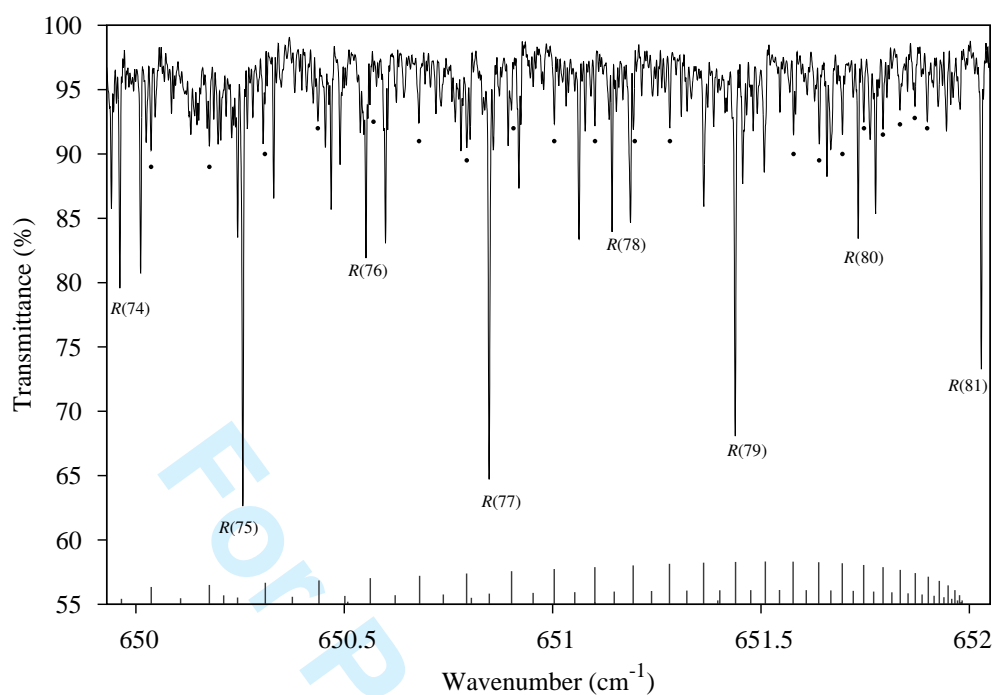


Figure 2. Infrared spectrum of diacetylene in the  $\nu_3 - \nu_9$   $Q$ -branch region. The stick spectrum shows the predicted positions and relative intensities of of the  $\nu_3 - \nu_9$  lines, whereas the filled dots indicate the assigned  $Q$ -branch transitions. Some features of the  $\nu_8$   $R$ -branch are also indicated.

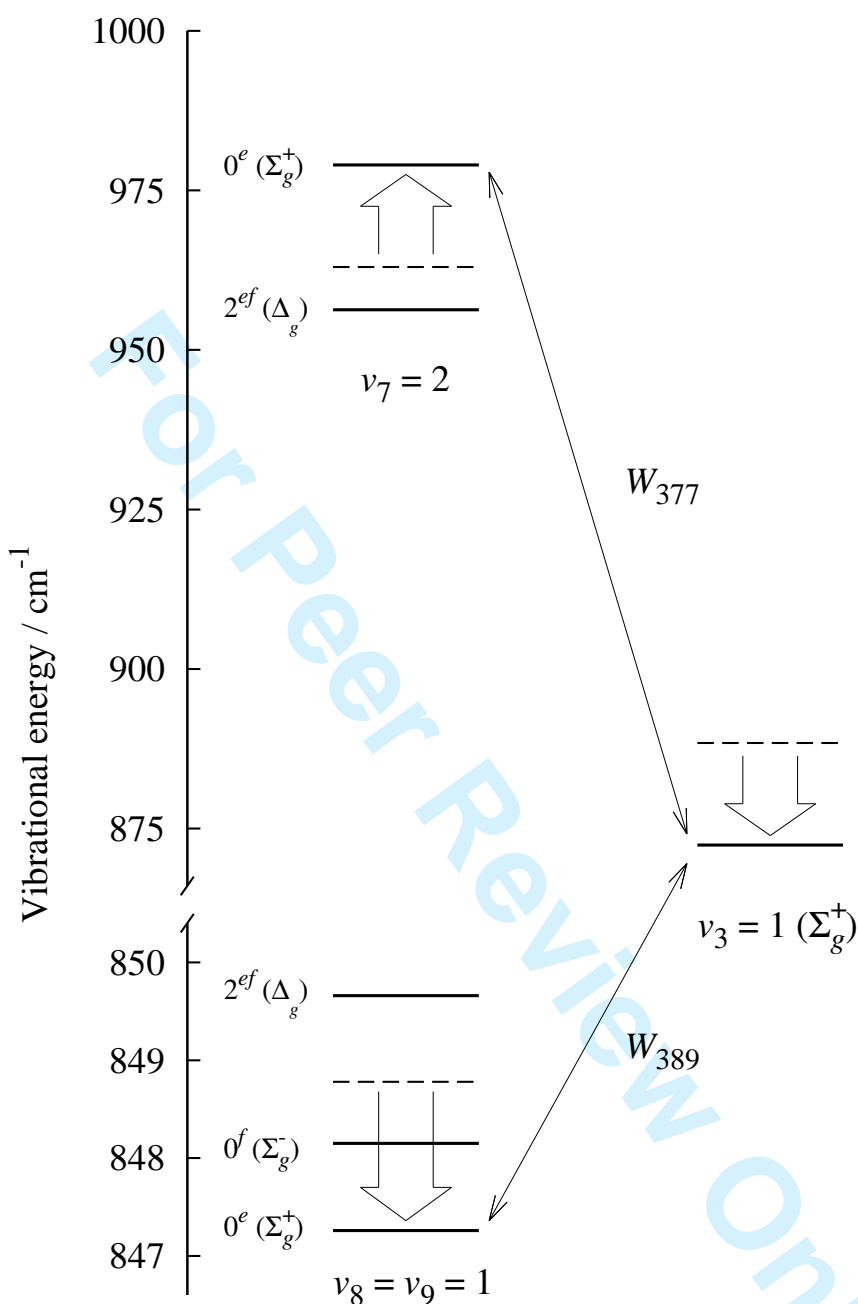


Figure 3. Vibrational energy level diagram of the three-state resonance system analysed for diacetylene. Dashed lines indicate the position of the unperturbed energy levels, the large arrows show the energy displacement produced by the anharmonic interaction. The diagram is not to scale.